CHAPTER IV
RESULTS AND DISCUSSION

4.1 Catalyst Characterization

The catalytic and physical properties of the $Au/CeO_2–ZrO_2$ catalysts was characterized by various techniques; XRD, BET, AAS, UV-vis, TPR, TEM, FT-IR, and FT-Raman in order to explain the changes in catalytic activities of PROX reaction.

4.1.1 Atomic Absorption Spectroscopy (AAS)

Atomic Absorption Spectroscopy was utilized to examine the actual gold loading of 1 wt% $Au/CeO_2–ZrO_2$, as summarizes in Table 4.1. The initial result showed that the actual gold loading was lower than the nominal Au loading due to non-attachment of gold complex anion ($[AuCl(OH)_3]^-$ and $[Au(OH)_4]^-$) on the support surface (Casaletto *et al.*, 2006). The amount of Au deposit on CeO_2 was higher than Au/ZrO_2. Moreover, for the use of $CeO_2–ZrO_2$ supports, the amount of Au deposit decreased with increasing Zr content. The possible explanation of these differences in Au deposition was that depended on point of zero charge (PZC) value of the support, which the PZC value for pure CeO_2 and ZrO_2 was approximate 7.72 and 4.87, respectively. If the PZC of the support is higher than the pH of the solution, the surface will be positive charge due to protonation of the surface hydroxyls, resulting in electrostatic adsorption of the gold anions. Whereas, the PZC of the support is lower than the pH of the solution, the surface will be negative charge due to the removal of protons from the surface hydroxyls, resulting in an electrostatic repulsion force of the gold anions (Chang *et al.*, 2009, Pojanavaraphan *et al.*, 2013). In the experiment, the pH of solution was adjusted to 8 for precipitation, which the pH was higher than PZC value of the support. Therefore, in case of mixed oxide support, the PZC value of $CeO_2–ZrO_2$ decreased with increasing the Zr content. The presence at lower PZC value had been

suggested than it had a stronger repulsive fore. Hence, it was agreement with the high gold loading was obtained for 1 wt% $Au/Ce_{0.75}Zr_{0.25}O_2$.

4.1.2 Surface Area

The surface areas of the 1 wt% $Au/Ce_{1-x}Zr_xO_2$ catalysts were illustrated in Table 4.1. The results showed that Au supported on pure ceria and zirconia supports gave the surface areas, which were 106.6 and 169.0 m^2/g, respectively. While the gold over mixed oxide supports had the surface areas in the range of 121.5–129.6 m^2/g, which were between those of individual supports. Among the $Au/CeO_2–ZrO_2$ catalysts, the surface area seemed to be increased with Zr addition in the mixed oxides, implying that the surface area of the catalysts was the consequences of the substitution of Ce^{4+} by Zr^{4+} ion (Zhang and Liu, 2013). It has been reported that the variation in Ce/Zr composition displayed the formation of $Ce_{1-x}Zr_xO_2$ solid solution, where the smaller Zr^{4+} ion can corporate and/or substitute inside the larger Ce^{4+} lattice to cause the shrinkage in both ceria lattice and crystallite size. This smaller ceria crystal led to the increment of the ceria (Reddy and Khan, 2005). As mention previously, it was reasonable to define the solid solution formation in the mixed oxide support as one of the main factors to improve the surface area. On the other hand, many studies reported that the substitution of zirconia in cerium structure slightly decreased their surface area (Dobrosz-Gómez *et al.*, 2008).

Table 4.1 Chemical-physical properties of the $Au/CeO_2–ZrO_2$ catalysts

Catalysts	Actual Au loading[a] (%)	Surface area[b] (m^2/g)	Average crystallite size[c] (nm)		Lattice constant[d] (nm)		I_{598}/I_{463}[e]
			CeO_2	Au (111)	CeO_2 (111)	CeO_2 (200)	
Fresh							
CeO_2	-	-	7.60	-	0.550	0.550	-
1 wt% Au/CeO_2	0.97	106.6	7.56	-	0.549	0.550	0.018
1 wt% $Au/Ce_{0.75}Zr_{0.25}O_2$	0.98	121.5	5.59	-	0.548	0.549	0.039
1 wt% $Au/Ce_{0.5}Zr_{0.5}O_2$	0.96	127.8	4.38	-	0.543	0.542	-
1 wt% $Au/Ce_{0.25}Zr_{0.75}O_2$	0.87	129.6	2.65	-	0.518	0.518	-
1 wt% Au/ZrO_{2z}	0.60	169.0	-	-	-	-	-
Spent							
1 wt% Au/CeO_2	-	-	7.60	-	0.544	0.544	0.290
1 wt% $Au/Ce_{0.75}Zr_{0.25}O_2$	-	-	5.83	-	0.544	0.547	0.072

All of samples were calcined at 400 °C.

[a] The percentage of each metal was measured quantitatively by AAS.

[b] The surface area was measured by BET.

[c] The mean crystallite sizes were calculated from the average values of CeO_2 plane (111), (200), (220), and (311).

[d] The unit cell parameters calculated from Bragg's equation.

[e] Calculated from the intensity ratio of Raman bands at 463 and 598 cm^{-1}.

4.1.3 UV-visible Spectroscopy

UV-visible spectroscopy is well known as the useful technique to identify Au species (Au^{3+}, Au cluster, and Au^0) of the catalyst and the results are presented in Figure 4.1. The pure CeO_2 and ZrO_2 showed the band around 370 nm and 208–210 nm, respectively. For the mixed oxide support observed the peak in the range of CeO_2 and ZrO_2 band. The adsorption band could be observed at 260–290 nm, according to the full connectivity of Ce–Zr–O linkages via by incorporation of Zr into the Ce lattice (Chen *et al.*, 2002, Pojanavaraphan *et al.*, 2013). Moreover, the peak of CeO_2 shifted to lower wavelength after adding Zr, which probably caused of Zr incorporation. Moreover, the peak of ZrO_2 strongly became visible at 209–240 nm at high ratio of Zr. From this could be implied that was possible to cause the formation of CeO_2–ZrO_2 solid solution.

The absorption band of gold clusters (Au_n, $1 < n < 10$) and gold metallic (or plasmon, Au^0) can be assigned at 280–300 nm (Souza *et al.*, 2008) and 500–600 nm (Park *et al.*, 2006), respectively. The cationic gold species (Au^{3+}) can be observed at lower 250 nm (Gangopadhayay and Chakravorty, 2004). The gold nanoparticles (Plasmon) appeared at 353 nm, but the gold clusters and cationic gold species were not clear to observe because the Au species also appeared the band in the range of oxide support. Therefore, it was difficult to assign the gold species on Au/CeO_2–ZrO_2 catalysts using UV-vis Spectroscopy. Furthermore, it observed the multiple peaks in the UV spectra that related to the charge transfer (CT) transitions, as illustrated in Table 4.2. For example, the band at 275–375 nm can be ascribed to $Ce^{4+} \leftarrow O_2$ while $Ce^{3+} \leftarrow O_2$ and/or $Zr^{4+} \leftarrow O_2$ charge transfer appeared at 228–275 nm (Kambolis *et al.*, 2010). Nevertheless, this technique can use to infer the change of mixed oxide, which could be attributed to the formation a solid solution. Moreover, the catalytic activity could relate to the gold species, which both Au^0 and Au^{3+} are important role for the activity (Wang *et al.*, 2007). From the results, Au/CeO_2–ZrO_2 had the coexistence of $Au^{\delta+}$ and Au^0 species on the support, which these only presented in qualitative analysis.

Table 4.2 Summary of UV-vis diffuse reflectance charge transfer band for CeO_2–ZrO_2 (Rao and Sahu, 2001)

Nature of species and transition	Wavelength (nm)
$O^{2-} \rightarrow Ce^{3+}$	255, 265, 250–350
$O^{2-} \rightarrow Ce^{4+}$	275, 278, 280, 250–350
$Ce^{3+} \rightarrow Ce^{4+}$	588, 650
Ce^{3+} species	205–208, 216–228
CeO_2	320–350, 370
Ce-O-Zr	260–290
$O^{2-} \rightarrow Zr^{4+}$	320–325
m–ZrO_2	209, 240, 308, 341–343, 351

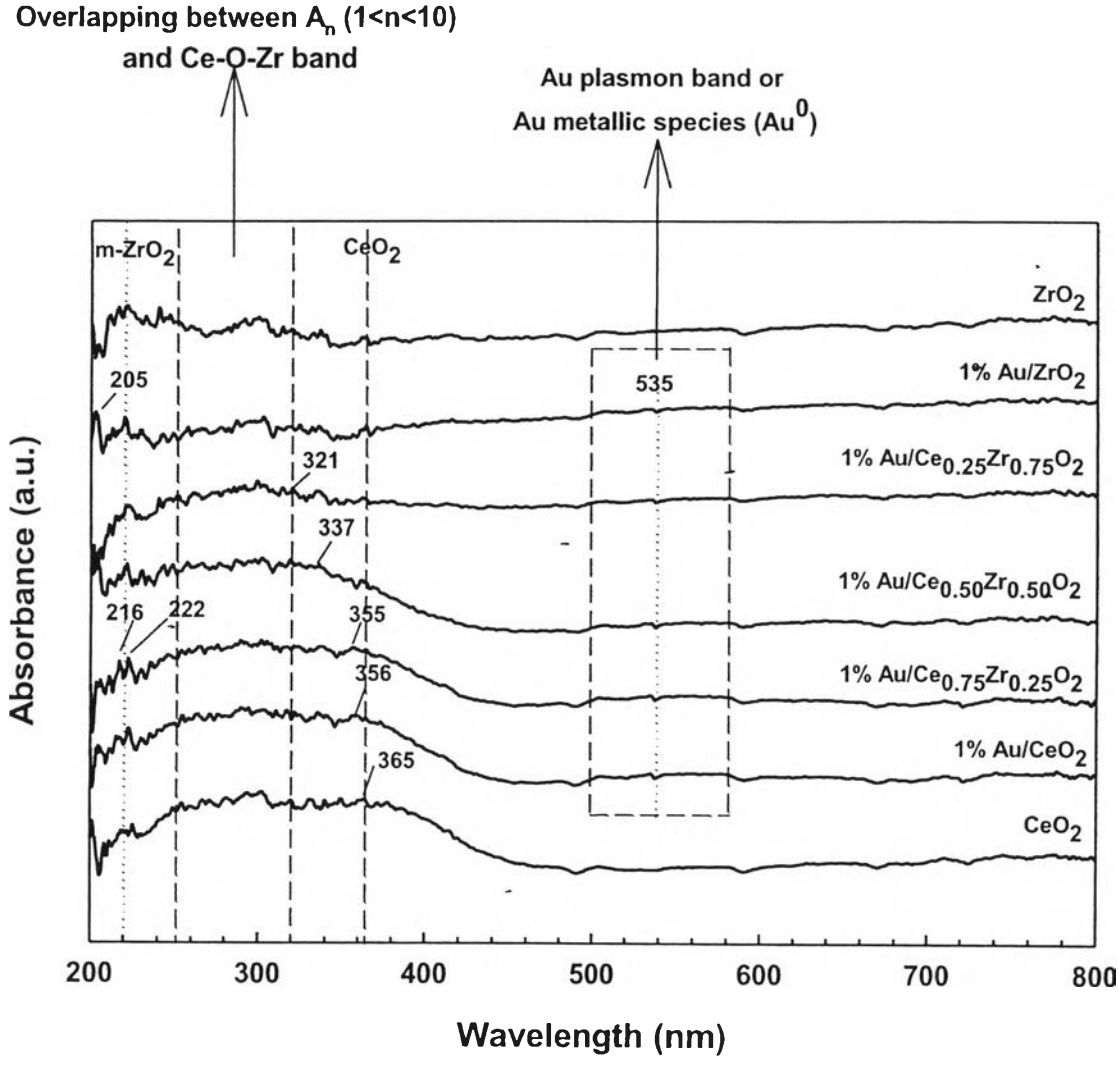

Figure 4.1 Diffuse reflectance UV-vis spectra of catalysts with various support compositions.

4.1.4 Temperature-Programmed Reduction (TPR)

The H_2–TPR profile was used to evaluate the reducibility of Au/CeO_2–ZrO_2 catalysts, as shown in Figure 4.2. The pure CeO_2 support presents two reduction peaks. The first reduction at low temperature (478 °C) is attributed to the reduction of oxygen on the ceria surface, and another higher temperature (836 °C) is related to bulk

reduction of $Ce^{4+} \rightarrow Ce^{3+}$. However, it was no observation of the ZrO_2 reduction in the range of studied temperature.

In the presence of Au, the appearances of the lowest reduction peaks at 77–100 °C was corresponded to the Au_xO_y species (or Au hydroxide) reduction (Dobrosz-Gómez *et al.*, 2010). For Au/CeO_2, it has been suggested that the role of gold modified the properties of ceria by enhancing the reducibility of CeO_2 surface oxygen, which probably caused to decrease the strength of the surface Ce–O bonds adjacent to gold atoms (Scire *et al.*, 2003). From this, it leaded to increase surface lattice oxygen mobility and reducibility. Moreover, the reduction peak of support also shifted to lower temperature, resulting from a strong interaction between metal and support (Chang *et al.*, 2008).

It is well-known that, the area of under the reduction peak can be related to the amount of reducible surface oxygen species. For example, if the area under the Au reduction peak is high, the amount of $Au^{\delta+}$ (Au^+ and Au^{3+}) species will be high for adsorbing the H_2 molecules during the reduction process. On the other hands, the low-reduction area can be inferred to a great number of Au^0 species, since Au^0 is normally less reductive than $Au^{\delta+}$, resulting in less H_2 consumption in the reduction process. When focusing on the change in Au reduction area with Zr content, it was found that the number of H_2 consumption (or area/intensity) decreased significantly after increasing the Zr content from 25% mole to 75% mole. This suggested that the generation of Au^0 species was more favorable with rich-Zr catalysts. To better understand the existence of Au^0 species at excess Zr^{4+} possibly dissolved inside the $Au^{\delta+}$ to form Au_n cluster or Au^0 specie (Chang *et al.*, 2008, Pojanavaraphan *et al.*, 2012). Not only the reduction area, but the position of the Au reduction peak also changed by shifting towards higher temperature (77 to 100 °C), which represented the strengthening of metal-support (Au-support) interaction. Hence, it was reasonable to speculate the changes in amount of Au^0 and Zr content as the consequences of Zr^{4+} solubility inside the $Au^{\delta+}$ after forming the strong interaction. However, the exact amounts of Au^0 and $Au^{\delta+}$ were not determined in

this study since the gap difference of the Au reduction area was large enough to briefly measure this species.

When correlating a variety of Au species to the catalytic activity, many literature have found that the active catalysts always contained metallic Au particles (Chang *et al.*, 2006) whereas the high activity of Au nanoparticle contained the coexistence of $Au^{\delta+}$ and Au^0 species (Han et al., 2009). In this work, both Au^0 and $Au^{\delta+}$ species acted as the catalytic active site, in which $Au^{\delta+}$ acted as a dominantly active species. Therefore, the combination of Au^0 and $Au^{\delta+}$ is responsible for the active sites in the reaction. The Au metallic activated the O_2 molecule and hydroxyl, which the gold cation (Au^{3+}) linked the Au metallic on the support and provide the pathway for the reaction (Sakwarathorn *et al.*, 2011), which is in agreement with the UV-vis analysis.

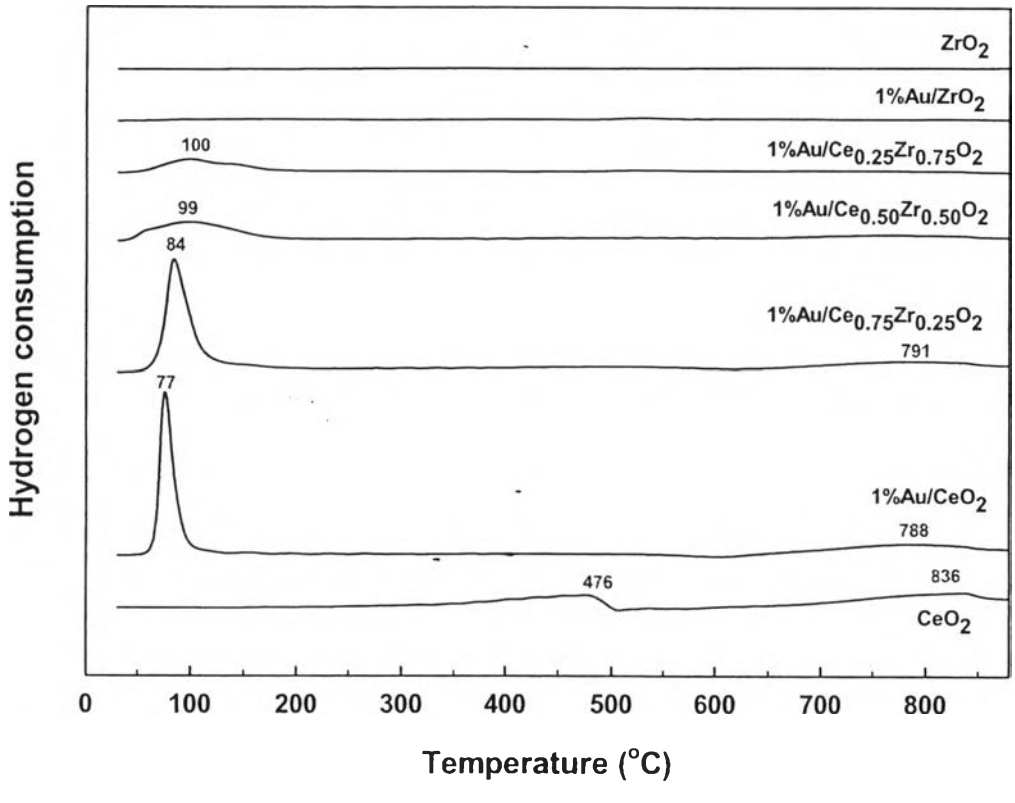

Figure 4.2 TPR profiles of the $Au/CeO_2–ZrO_2$ catalysts with various support compositions.

4.1.5 X-ray Diffraction (XRD)

The XRD patterns of 1 wt% $Au/Ce_{1-x}Zr_xO_2$ supports are presented in Figure 4.3, and the XRD pattern of CeO_2 supported presented the characteristic of face centered cubic (FCC), fluorite type structure. For the ZrO_2 support, it presents mainly monoclinic and tetragonal phases. Eight diffraction peaks of ceria were detected; 28.46°, 32.97°, 47.38°, 56.24°, 58.78°, 69.20°, 76.56°, and 78.77°, which were indexed to (111), (200), (220), (311), (222), (400), (331) and (420) crystal faces (Dobrosz-Gómez *et al.*, 2008, Zhang and Liu, 2013). It was clearly seen that the CeO_2 diffractions slightly shifted to higher angles, and the peaks became broader with lower intensity after increasing the amount of Zr concentration. This evidenced the corporation of Zr^{4+} cation (radius 0.84 Å) inside the Ce^{4+} (radius 0.97 Å) lattice to form the $Au/Ce_{1-x}Zr_xO_2$ solid solution phase. Our results were in agreement with many previous works, which found the defects or distortions in the in the oxygen sublattice of ceria after adding more Zr contents (Rodriguez *et al.*, 2003).

This changing behavior of CeO_2 diffraction resulted in the decrease in the average crystallite size and ceria lattice constant from 7.52 to 2.65 nm and from 0.549 to 0.518 nm, respectively (Table 4.1). Again, these results could confirm the formation of solid solution phase which led to the shrinkage in ceria lattice distance after Zr^{4+} incorporation (Reddy and Khan, 2005, Zhang and Liu, 2013). Moreover, the smaller crystallite size was in line with the increasing of BET surface area (Dobrosz-Gómez *et al.*, 2008). It was believed that this incorporation can enhance the formation of vacancies in the anion sublattice during the charge balancing, where the redox properties in ceria can be improve. Interestingly, the ZrO_2 diffractions became visible at the rich-Zr catalysts (1 wt% $Au/Ce_{0.5}Zr_{0.5}O_2$ and 1 wt% $Au/Ce_{0.25}Zr_{0.75}O_2$). This might represent the non-uniform solid solution phase, where some of ZrO_2 particles possibly remained on the catalyst surface, not being favorable to incorporation inside the ceria lattice. This was probably found in the use of excess Zr concentrations. While the use of lean Zr concentration (1 wt% $Au/Ce_{0.75}Zr_{0.25}O_2$) showed no observation of ZrO_2 diffraction, which represented the most uniform solid solution phase or the ZrO_2 was highly disperse

on the catalyst surface. Nonetheless, the Au diffraction phase (111) at 38.5° was not detectable for all catalysts, suggesting either well-dispersed of gold nanoparticles on the support or low amount of gold deposition (Wang *et al.*, 2007, Vicario *et al.*, 2009).

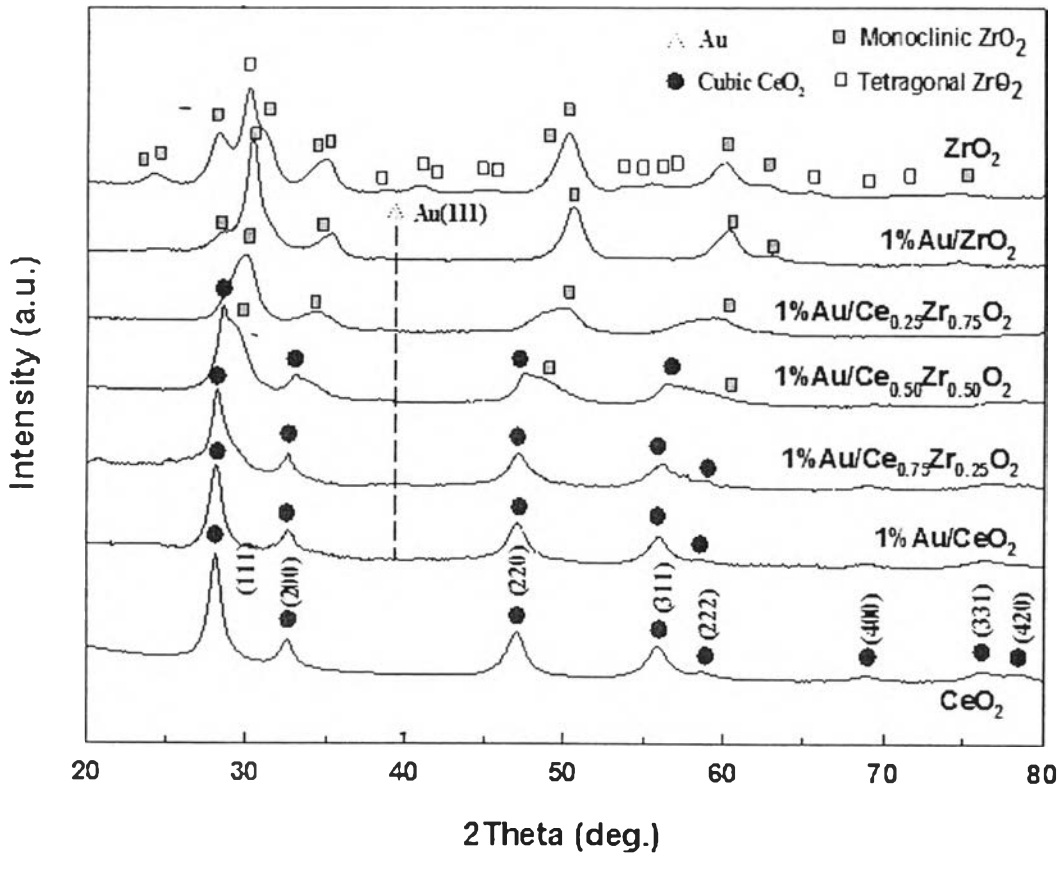

Figure 4.3 XRD patterns of supported Au catalysts.

Table 4.3 CeO_2 and Au crystallite sizes of the 1 wt% Au catalysts over different supports

Catalysts	Crystallite size (nm)				
	$CeO_2(111)$	$CeO_2(200)$	$CeO_2(220)$	$CeO_2(311)$	Au(111)
CeO_2	9.01	8.84	6.31	6.05	-
1 wt% Au/CeO_2	9.08	8.18	6.43	6.33	-
1 wt% $Au/Ce_{0.75}Zr_{0.25}O_2$	6.10	6.14	4.46	5.66	-
1 wt% $Au/Ce_{0.5}Zr_{0.5}O_2$	6.02	4.31	3.02	4.18	-
1 wt% $Au/Ce_{0.25}Zr_{0.75}O_2$	4.33	3.21	3.05	2.31	-
1 wt% Au/ZrO_2	-	-	-	-	-
ZrO_2	-	-	-	-	-

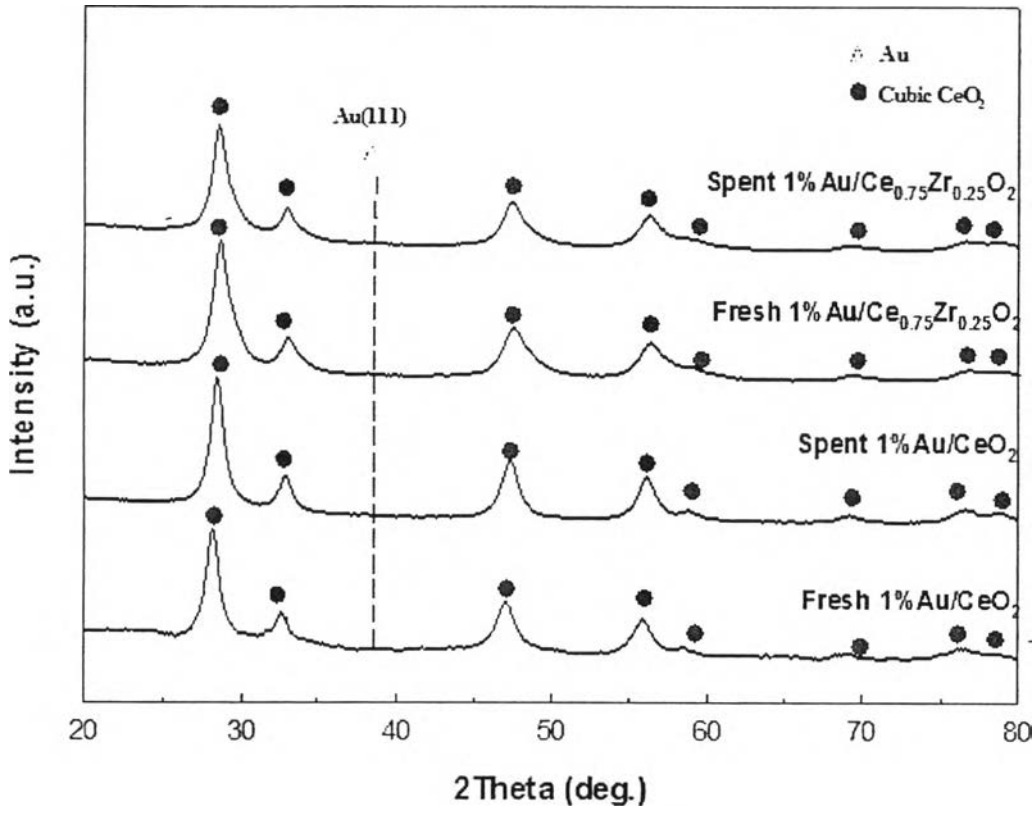

Figure 4.4 XRD patterns of fresh and spent of 1 wt% Au/CeO_2 and 1 wt% $Au/Ce_{0.75}Zr_{0.25}O_2$.

Figure 4.4 illustrates the comparison of XRD patterns between the fresh and spent 1 wt% Au/CeO_2 and 1 wt% $Au/Ce_{0.75}Zr_{0.25}O_2$ after exposure to the reaction for 33 hours. The spent catalyst had almost the same XRD pattern as that of fresh catalyst, implying that there was no change in the crystallite structure of both Au and CeO_2 (Gluhoi *et al.*, 2005). However, the spent catalyst had larger average ceria crystallite size from 7.56 to 7.60 nm and 5.59 to 5.83 nm for 1 wt% Au/CeO_2 and 1 wt% $Au/Ce_{0.75}Zr_{0.25}O_2$, respectively. The Au reflection peak was not observed in the both fresh and spent catalysts.

Taking into account the lattice constants of the spent catalysts both 1 wt% Au/CeO_2 and 1 wt% $Au/Ce_{0.75}Zr_{0.25}O_2$ showed the decrease in the lattice constants from 0.550 to 0.544 nm and 0.548 to 0.545 nm, respectively. It had been suggested that the gas feeding stream possibly affected on the variation in ceria lattice, where the ceria lattice varied significantly with an increase after exposure to CO and a decrease after exposure to H_2O (Wang *et al.*, 2006). Therefore, it could be related to the complex mechanisms during the reaction that changed the ceria lattice and helped restructure the solid solution phase. However, the exact mechanism was still unclear for the solid solution recovery.

4.1.6 Raman Spectroscopy

Figure 4.5 shows the Raman spectra of the fresh and spent catalysts for Au/CeO_2 and $Au/Ce_{0.75}Zr_{0.25}O_2$. The main band at 463 cm^{-1} was corresponded to the oxygen breathing vibrations around each Ce^{4+} in metal oxides (F_{2g} mode), and the weak band around at 598 cm^{-1} is associated to the formation of oxygen vacancies in the ceria lattice (Reddy and Khan, 2005, Hernández *et al.*, 2010). The ZrO_2 bands typically appeared at 176, 380, 475, and 640 cm^{-1} for monoclinic phase and 266, 313, 470, and 640 cm^{-1} for tetragonal phase (Maia *et al.*, 2012). In case of Zr incorporation, the Raman frequency shifted to higher wave numbers, which the intense bands attributed to the overlapping of ceria and zirconia phase and it also appeared the weak bands of zirconia around 380 and 313 cm^{-1}. Furthermore, the shift of the band to higher frequency and

less sharp of the band is related to the decreasing crystallite size or lattice constant (Neto and Schmal, 2013), which these results confirm the formation of a solid solution, in accordance with previous XRD results.

In addition, the intensity ratio of the band of oxygen vacancies and the F_{2g} mode of fluorite-type structure (I_{598}/I_{463}) was also calculated to evaluate the amount of oxygen vacancies of a sample, as shown in Table 4.1. The intensity ratio increased with incorporation of Zr , implying that the doping of Zr in CeO_2 increased the concentration of oxygen vacancies due to the change of lattice of CeO_2 by substitution of Ce^{4+} with Zr^{4+}. From this change caused to promote the lattice deformation and formation of oxygen vacancies. In general, an oxygen vacancy is produced by the reduction of the cationic Ce^{4+} to Ce^{3+}. The addition of smaller Zr^{4+} could provide some spare space for accommodating the bigger Ce^{3+} cations and increase the formation of an oxygen vacancy (Grau-Crespo *et al.*, 2011).

Moreover, the intensity ratio of fresh catalysts was also compared with spent catalysts. It was found that the ratio increased after the stability test, indicating that it may occur some defect structure or restructure during the reaction (Pojanavaraphan *et al.*). From this defect caused to change the lattice and increased the amount of oxygen vacancies. Therefore, the evidence from Raman and XRD data revealed a change of CeO_2 lattice in the presence of Zr according to the formation of solid solutions and increase the number of oxygen vacancies. On the other hand, the reduction of an oxide causes the formation of surface vacancies, which then migrate into the bulk. The reduction progressively empties the surface of active Ce^{4+} sites, which would limit the oxygen available for reduction. Although, the catalyst surface was created more oxygen vacancies, they cannot diffuse O^{2-} in the lattice, according to rate-determining step (Boaro *et al.*, 2000). It can be implied that the high oxygen vacancies didn't mean the high activity due to limitation of oxygen storage capability.

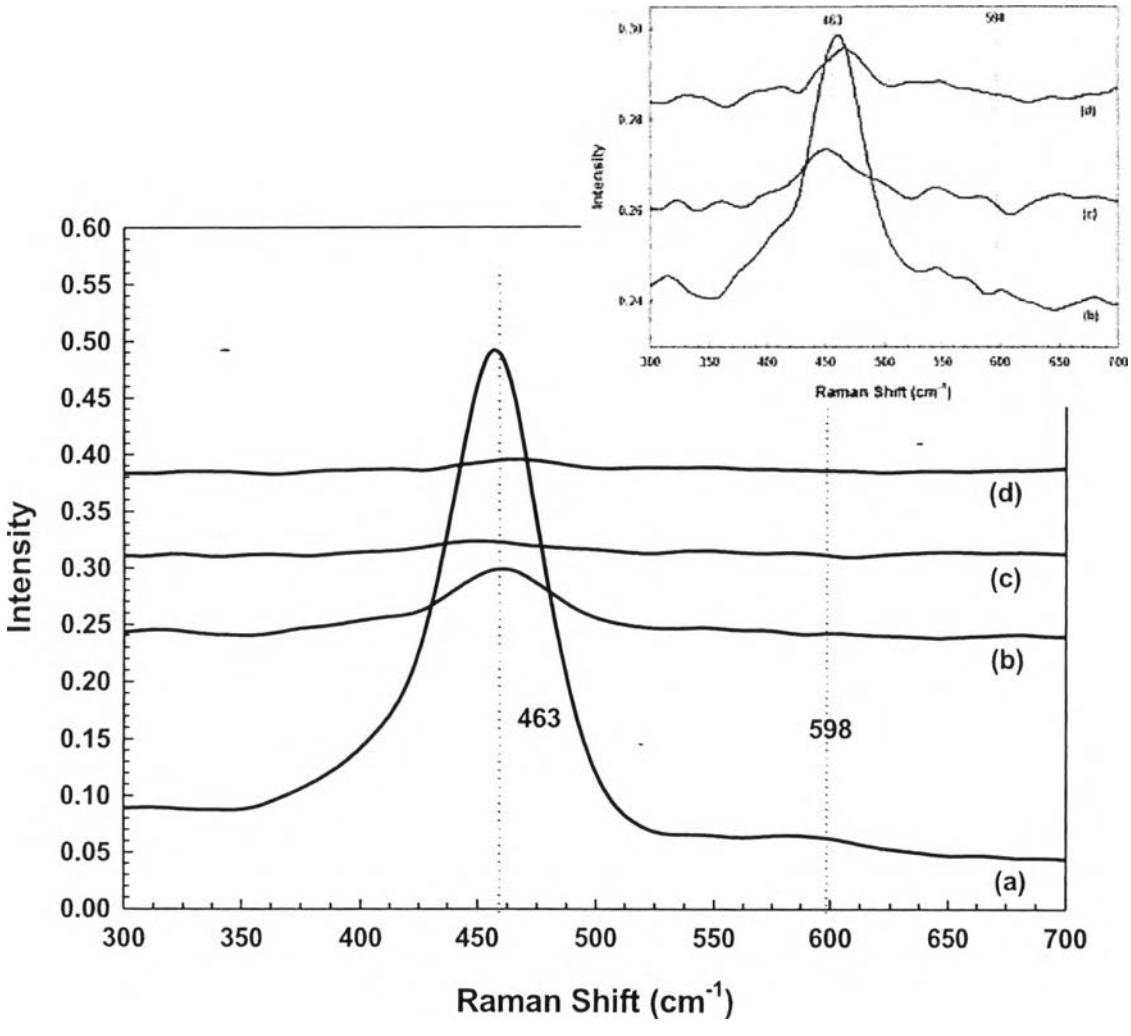

Figure 4.5 Raman spectra of 1 wt% $Au/CeO_2–ZrO_2$ catalysts for (a)1 wt% Au/CeO_2–fresh (b) $Au/Ce_{0.75}Zr_{0.25}O_2$–fresh (c) Au/CeO_2–spent (d) $Au/Ce_{0.75}Zr_{0.25}O_2$–spent.

4.1.7 Fourier Transform Infrared Spectroscopy (FT-IR)

FT-IR used to determine the functional groups on the surface of the fresh and spent catalysts, are shown in Figure 4.6. FTIR spectra were observed in two regions, which a broad band region was O-H stretching mode at the wave number range of 2500–3700 cm^{-1} (Gamarra and Martínez-Arias, 2009). The second region was at the wave number range of 1200–1800 cm^{-1}, which corresponded to the chemisorption carbonate species (Fan *et al.*, 2008). After the catalyst was tested in a simulated wet condition (with H_2O + CO_2), the intensity of O–H peak at 3400 cm^{-1} was higher and broader than the fresh catalyst. It may cause from the presence of undissociated water molecules or the hydrogen produced amount of water on the surface catalyst. The spent catalysts also showed a strong peak at 1343 cm^{-1}, according to the CO molecules adsorbed on the surface by chemisorption. The formation of carbonates is an indication of CO oxidation by surface oxygen species and it presented the band at 1582, 1413, and 1220 cm^{-1}, which assigned to bicarbonate species (HCO_3^-) (Boccuzzi *et al.*, 1999). The band at 1640 cm^{-1} corresponding to O-H bending mode of molecular water are observed. Moreover, the band at 2351 cm^{-1} can be observed and it typically assigned to gaseous CO_2 due to CO_2 molecules linearly adsorbed on the surface cations of the support (Boccuzzi *et al.*, 1999). It also appeared the band at 2840 and 2940 cm^{-1} that corresponded to the formation of the formate species on the catalyst surface (Gamarra and Martínez-Arias, 2009). In addition, the spent catalyst was compared in the different operating temperature. It showed that at low temperature had a stronger accumulation of both carbonate and formate species than high temperature. This suggested that these species decreased at the temperature above 100 °C (Gamarra and Martínez-Arias, 2009). Thereby, the temperature has a significant effect on the catalytic activity.

Figure 4.7 illustrates the FTIR spectra of spent catalysts after exposure the WGS reaction for 1 wt% Au/CeO_2 and 1 wt% $Au/Ce_{0.75}Zr_{0.25}O_2$. It can be observed that Au/CeO_2 had high amount of carbonate/bicarbonate species than $Au/Ce_{0.75}Zr0_{.25}O_2$. These species was formed during the reaction due to the carbonate-like species are the main intermediates in WGS reaction (Costello *et al.*, 2003). It has been suggested that

the accumulation of carbonate species attributed on the acid-base properties of the supports , which the acid support was less adsorption of carbonate-like species and had more resistant to deactivation by these species than the base support (Vindigni *et al.*, 2012, Sudarsanam *et al.*, 2014). Thus, the incorporation of Zr could enhance the acidic properties of CeO_2, which could be easily to remove the surface carbonates.

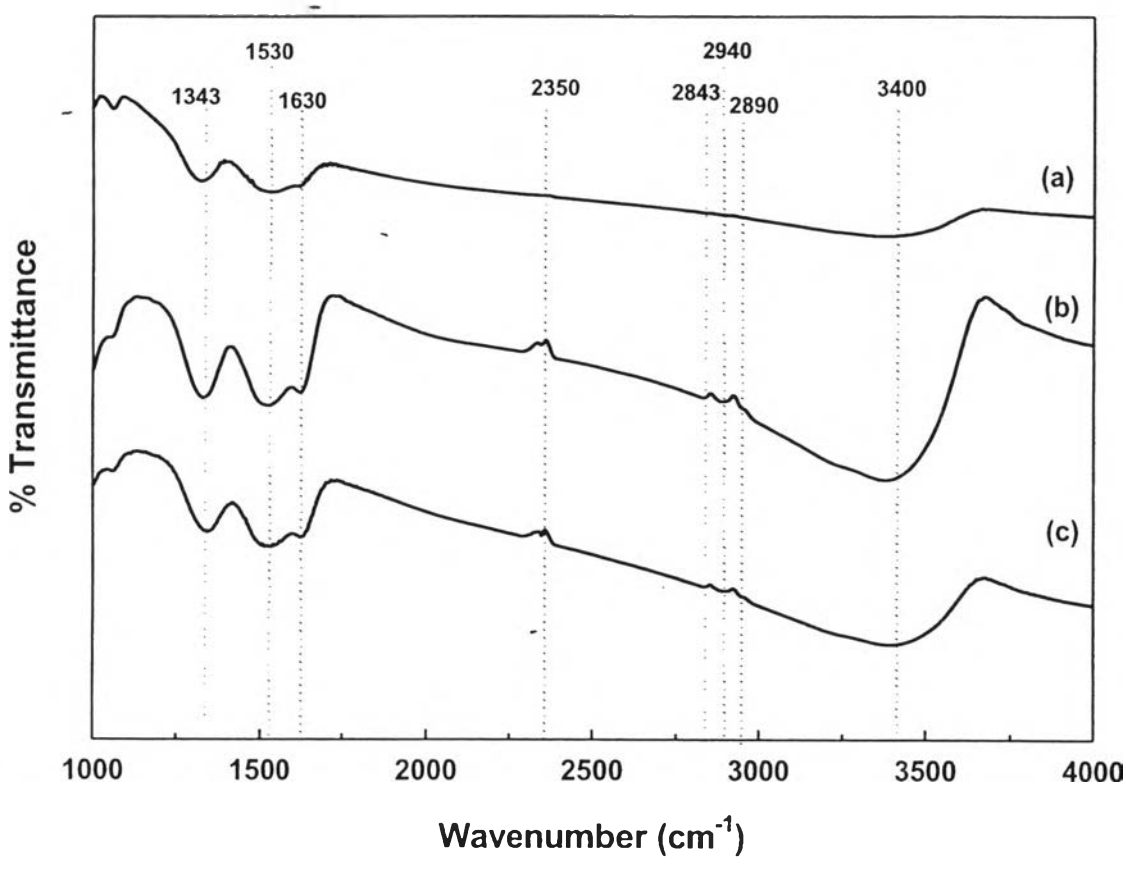

Figure 4.6 FTIR spectra of 1 wt% $Au/Ce_{0.75}Zr_{0.25}O_2$ catalysts; (a) fresh catalyst, (b) spent catalyst after exposure at 50 °C, and (c) spent catalyst after exposure at 110 °C with gas composition of 40% H_2, 1% O_2, 1% CO, 10% CO_2, and 10% H_2O in He.

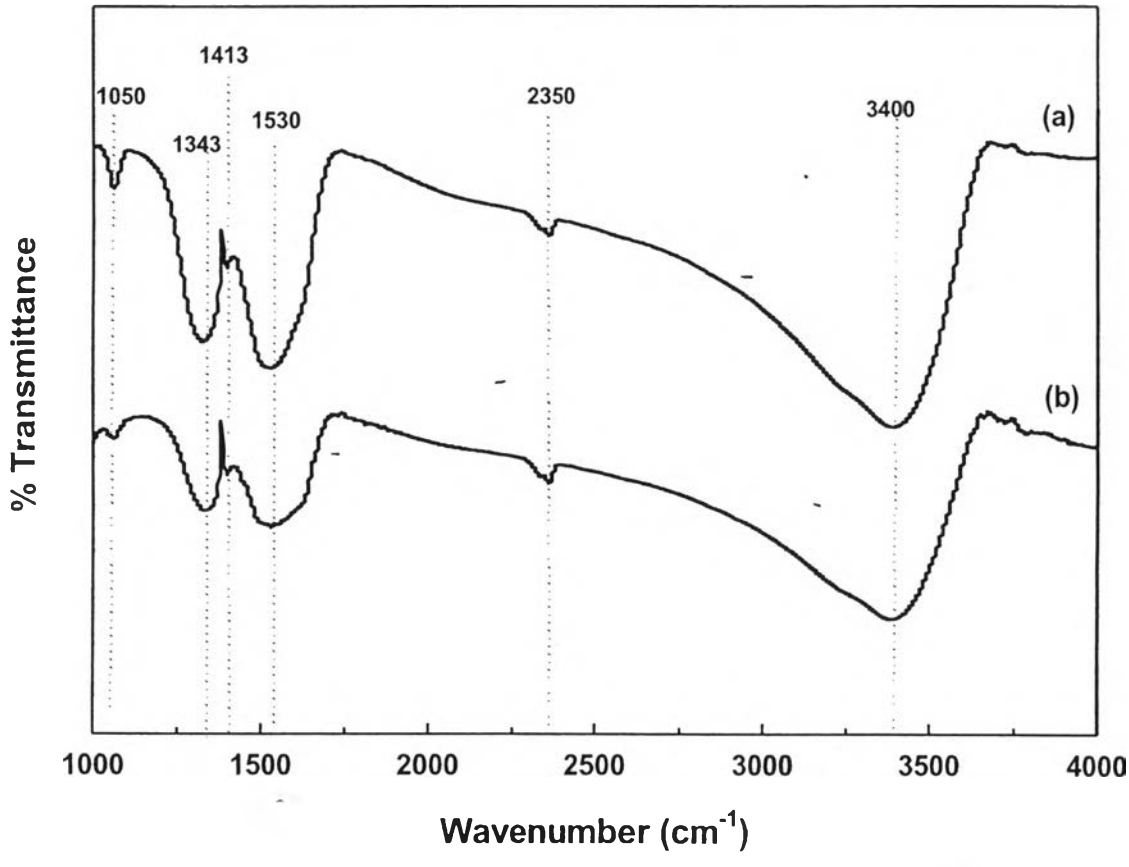

Figure 4.7 FTIR spectra of spent catalysts in WGS reaction; (a) 1 wt% Au/CeO_2 , (b) 1 wt% $Au/Ce_{0.75}Zr_{0.25}O_2$.

Table 4.4 Summary of frequency and assignment of carbonate, formate, and intermediate bands of fresh and spent 1 wt% $Au/Ce_{0.75}Zr_{0.25}O_2$ (Tabakova *et al.*, 2003)

Wavenumber (cm^{-1})	**Assignment**
1045–1070, 1200–1800	Carbonate species
1220, 1413, 1530, 1582	Bicarbonate species
1343	CO molecules adsorbed on the surface
1630	Bending mode of undissociated H_2O
2350	Linear CO_2 weakly interacting with ceria
2840–2940	Formate species
2500–3700	O–H stretching mode

4.2 Catalytic Activity

In this part, the catalytic activity of the catalysts was examined in preferential CO oxidation. The catalytic activity was carried out at atmospheric pressure in a fixed-bed reactor containing 100 mg of catalyst in 80–120 mesh size. The reactant gas containing 1% CO, 1% O_2, 40% H_2 with He balanced was passed through the reactor with a total flow rate of 50 ml/min at the temperature range of 50 to 190 °C.

4.2.1 Effect of Support Composition on the Catalytic Activity

The effect of support composition on 1% wt $Au/Ce_{1-x}Zr_xO_2$ (x = 0, 0.25, 0.5, 0.75, 1) was varied. The catalysts were synthesized by co-precipitation technique and then 1% wt Au was deposited on the prepared support by deposition-precipitation technique. Figure 4.8 illustrates the catalytic activity in terms of CO conversion and selectivity towards CO oxidation of 1% wt $Au/Ce_{1-x}Zr_xO_2$ catalysts with various support atomic ratios.

From Figure 4.8, it can be seen that the catalytic activity depended on Ce/Zr atomic ratio of the oxide support. The results showed that 1 wt% Au/CeO_2 and 1 wt% $Au/Ce_{0.75}Zr_{0.25}O_2$ had a similar catalytic performance that they had high activity at low temperature then the activity decreased with increasing temperature. Whereas the activity of 1 wt% $Au/Ce_{0.5}Zr_{0.5}O_2$, 1 wt% $Au/Ce_{0.25}Zr_{0.75}O_2$, and 1 wt% Au/ZrO_2 increased with increasing temperature until they reached maximum CO conversion, after that the activity began to decrease. Due to a higher temperature, there is decrease in selectivity, regarding higher activation energy for the H_2 oxidation than for the CO oxidation (Luengnaruemitchai *et al.*, 2004) and in case of rich Ce-content gave a stable in selectivity with the operating temperature.

The maximum CO conversions were 92.36% (with 48.37% selectivity) for 1 wt% Au/CeO_2 at 50 °C, 94.06% (with 49.09% selectivity) for 1 wt% $Au/Ce_{0.75}Zr_{0.25}O_2$ at 50 °C, 85.58% (with 42.35% selectivity) for 1 wt% $Au/Ce_{0.5}Zr_{0.5}O_2$ at

70 °C, 61.70% (with 30.45 selectivity) for 1 wt% $Au/Ce_{0.25}Zr_{0.75}O_2$ at 90 °C, and 53.71% (with 31.51% selectivity) for 1 wt% Au/ZrO_2 at 90 °C.

Form the results indicated that the role of a support had an effect on the catalytic performance. Therefore, the catalytic activity of the catalysts can be ordered 1 wt% $Au/Ce_{0.75}Zr_{0.25}O_2 \geq$ 1 wt% Au/CeO_2 > 1 wt% $Au/Ce_{0.5}Zr_{0.5}O_2$ > 1wt% $Au/Ce_{0.25}Zr_{0.75}O_2$ > 1 wt% Au/ZrO_2. The incorporation of zirconium was beneficial for the enhancement of oxygen mobility (Lin *et al.*, 2009). However, the performance of the catalyst depended on an appropriate amount of zirconium content. In this work, 1 wt% $Au/Ce_{0.75}Zr_{0.25}O_2$ was slightly more activity than 1 wt% Au/CeO_2 at high temperature. It had been revealed that the $Ce_{1-x}Zr_xO_2$ composite with a low Zr-content exhibited good oxygen storage capacity and high oxygen mobility (Zhao *et al.*, 2011).

Consequently, the highest activities for 1 wt% $Au/Ce_{0.75}Zr_{0.25}O_2$ could be attributed that a solid solution may improve the catalytic activity and increase the oxygen vacancies, as confirmed by XRD and FT-Raman results. The presence of oxygen vacancies allowed effective O_2 adsorption and activation for CO oxidation (Longo *et al.*, 2012). Therefore, the $Ce_{1-x}Zr_xO_2$ composite with a low Zr content exhibited a large amount of oxygen vacancies that the pure CeO_2, which was found to enhance in oxygen mobility and promoted a high oxygen storage capacity. In addition, it had the presence the highest amount of Au deposited on the support that may promoted the reaction. So, the catalyst should have appropriate composition to employ the optimum catalytic performance. Furthermore, the catalytic performance could attribute to the gold species of the catalyst, which both Au^0 and Au^{3+} are responsible for the activity (Wang *et al.*, 2007). In this work, the 1% wt $Au/Ce_{0.75}Zr_{0.25}O_2$ exhibited the highest activity with coexistence of $Au^{\delta+}$ and Au^0 species on the support.

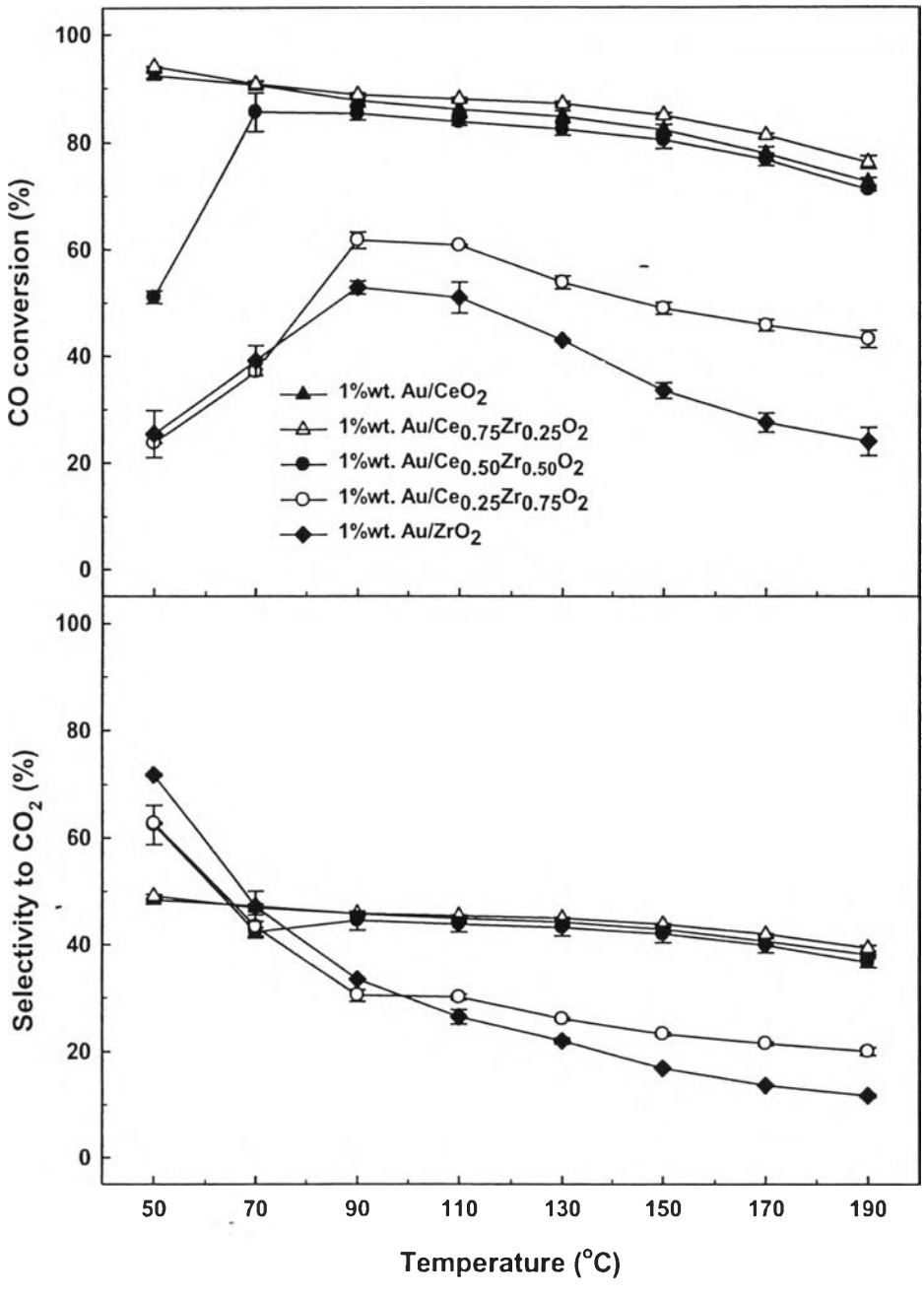

Figure 4.8 CO conversion and selectivity to CO_2 as a function of reaction temperature for PROX reaction over 1 wt% Au/CeO_2–ZrO_2 catalysts with various atomic ratios of Ce/Zr.

4.2.2 Effect of Additional Feed Stream Composition on the Catalytic Activity

Normally, the hydrogen-rich stream from reforming gases contains some amount of H_2O and CO_2. Therefore, the study on the catalytic activity of H_2O and CO_2 in the feed stream are very interesting. The presence of CO_2 and H_2O in H_2 streams originating from a reforming process is significant, and their effect on catalyst performance was studied by addition of either CO_2 or H_2O to the feed stream. The 1 wt% Au/CeO_2 and 1 wt% $Au/Ce_{0.75}Zr_{0.25}O_2$ catalysts were tested with the reformate gas composition (1% CO, 1% O_2, 40% H_2, 0–10% H_2O, 0–10% CO_2, and balanced in He). The coadsorption of H_2O and CO_2 can cause the severe effect for the catalyst due to the blockage of the active sites on the surface of catalysts (Zhao et al., 2011). Besides, the reaction temperature had the significant impact on the catalytic performance, which it depended on the nature of the catalyst.

4.2.2.1 Effect of Temperature in the Presence of CO_2 and H_2O

Figure 4.9 presents the effect of reaction temperature in the presence of 10% CO_2 and 10% H_2O on CO conversion and selectivity of 1 wt% $Au/Ce_{0.75}Zr_{0.25}O_2$ catalyst under different condition. From the range of both the temperature reaction (50-190 °C), the highest activity was obtained at 50 °C and it is an interesting to investigate at 110 °C because this temperature is close to the operating condition of PEMFCs. Moreover, it had been suggested that in the presence of water addition to the feed stream, at the temperature higher than 100 °C, a high CO conversion was obtained (Daté *et al.*, 2002). It was reported that at high temperature, a higher activity was obtained the best results than low temperature since it may not be achieved from the water gas shift reaction ($H_2O + CO \leftrightarrow H_2 + CO_2$) (Schubert *et al.*, 2004). On the other hand, some work obtained the best result at low temperature (Naknam *et al.*, 2009). In this experiment, the reaction was investigated at a constant temperature of 50 °C and 110 °C with time-on-stream. It was found that the temperature had significant effect on the performance both CO conversion and selectivity. The reaction temperature at 50 °C was significantly low CO conversion when compared to the results of temperature at 110 °C under presence of H_2O and CO_2 but increased the selectivity. In the case of H_2O, CO

conversion dramatically decreased at low temperature, whereas at high temperature gave a same result as normal feed stream. The CO conversion also rapidly dropped with adding CO_2 to the feed stream for both temperature, but it was higher impact effect at low temperature. When adding both CO_2 and H_2O, they were a significantly negative impact on the catalytic activity at low temperature, which CO_2 had more negative effect than H_2O. Although, the selectivity was increased at 50 °C, O_2 conversion was lower than 110 °C. So, O_2 consumption in conversion CO to CO_2 was less at low temperature and selectivity has not effect much to the activity when compared with CO conversion. The water vapor may be condensed on the catalyst surface, which may block the active site. On the other hand, CO molecules seem to be desorbed and allowed O_2 to adsorb for the reaction (İnce *et al.*, 2005) at high temperature. In case of water, it will dissociate to form OH, and it reacts with CO to produce HCOO. Then the formate decomposes to H_2 and CO_2 products (Boccuzzi *et al.*, 1999). It might be not achieved to decompose the formate species and became to block the active sites at low temperature. Thus, these catalysts flavored the reaction at high temperature in case if additional feed stream condition. Furthermore, the evidence in the FTIR spectra confirmed that the formation of carbonate and formate species was higher at low temperature. Therefore, the accumulation of these species could block the active sites and had a significant effect on the catalytic performance for the PROX reaction.

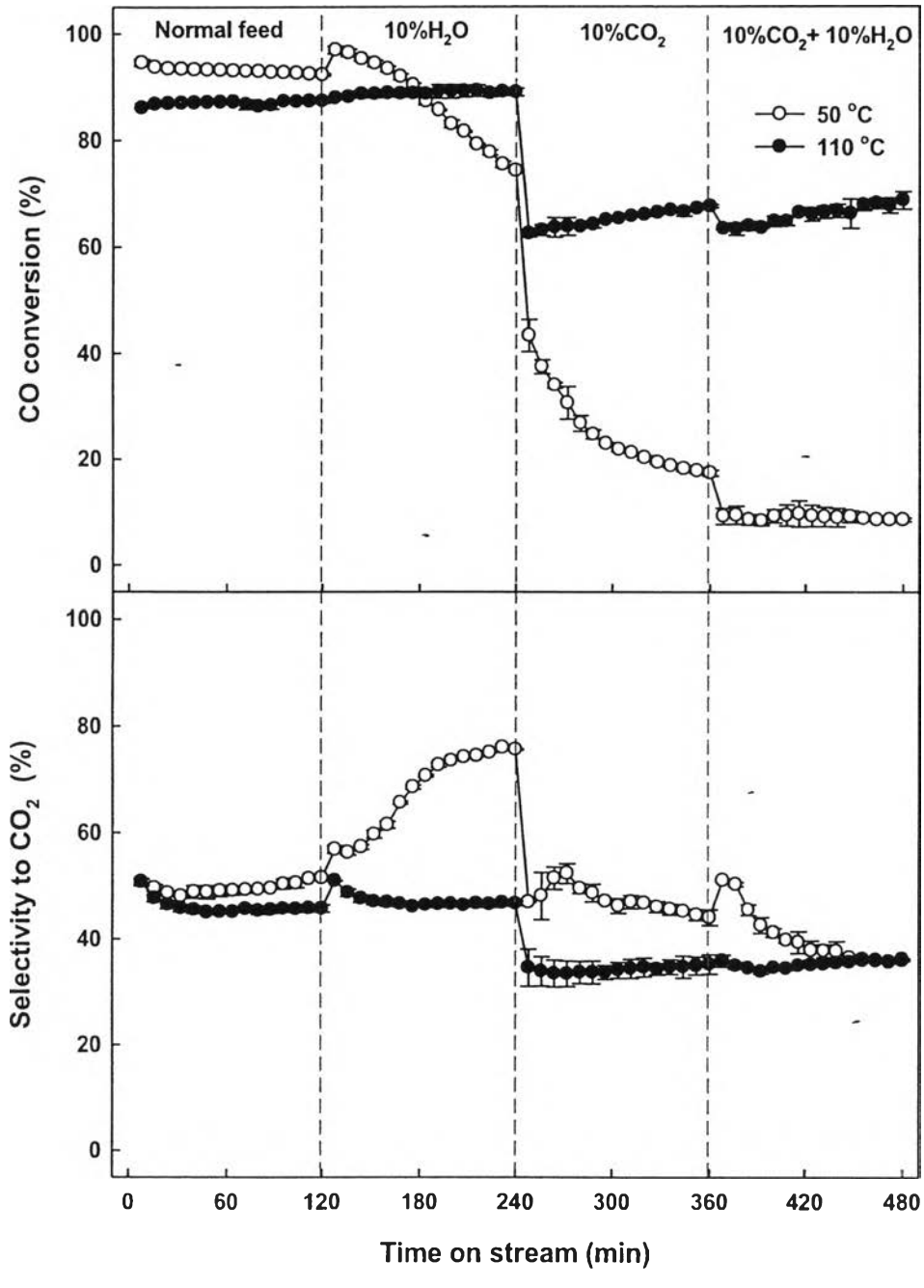

Figure 4.9 Effect of temperature in the presence of 10% CO_2 and 10% H_2O on the catalytic activities of 1 wt% $Au/Ce_{0.75}Zr_{0.25}O_2$. The reaction was tested at constant temperature of 50 °C and 110 °C and monitored with time-on-stream.

4.2.2.2 Effect of Water Vapor

With 10% of H_2O was added into the reactant feed stream. From Figure 4.10 can be observed that it obtained quite similar activity with the normal feed condition and gave a small increase with the reaction time. Many work proposed that addition of water favored for CO oxidation reaction because it could supply hydroxyl group that may promote the reaction by activating molecular oxygen on the surface or it may help to decompose the carbonates species on the catalyst surface (Ojifinni *et al.*, 2008). So, it was observed that the presence of water had no effect on the performance of both catalysts. In contrast, some groups observed that the presence of water vapor had a negative effect on the performance of the catalyst due to blocking of water on the active sites by adsorbed water on the catalyst surface (Schubert *et al.*, 2004).

4.2.2.3 Effect of CO_2 Addition

With 10% of CO_2 was added into the reactant feed stream, the results showed that the maximum CO conversion dropped from ~90% to ~65% conversion and the selectivity dropped from ~46% to ~34% (Figure 4.10). Several experimental studies have proved that existence of carbonate species on the surface of Au catalysts could block the active sites essential for CO oxidation. Adding of CO_2 had severe negative effect on the catalytic performance due to blocking the active sites by formation of carbonate, which inhibited the oxygen mobility as well as the competitive adsorption of CO and CO_2 on the surface of catalyst (Park *et al.*, 2004, Marino *et al.*, 2005). Another aspect, it occurred the reverse water-gas shift that may lower the CO conversion ($H_2 + CO_2 \rightarrow H_2O + CO$) (Zhao *et al.*, 2011). Therefore, CO_2 containing was responsible for catalyst deactivation and it significantly reduced the activity of the catalysts.

4.2.2.4 Effect of Combination H_2O and CO_2

With combination of 10% H_2O and 10% CO_2 were added to the reactant feed, as shown in Figure 4.10. Many work had been found that adding H_2O with CO_2 could improve the catalytic activity than adding only CO_2 because water can provide the OH–group to take place the reaction (Schubert *et al.*, 2004). However, in the

presence work obtained the negative results with adding both H_2O and CO_2 in the feed stream. The CO conversion and selectivity reduced from ~90% to ~65% and 46% to 34%, respectively. Both H_2O and CO_2 together could create the blockage of the active sites of the catalyst by carbonate and formate species. This may be attributed to the reverse water gas shift (Wu *et al.*, 2013) and the negative effect of CO_2 was more dominant than the positive effects of H_2O. Therefore, the catalytic activity trend becomes bad for the combination feeding of H_2O and CO_2 with the reactant gas.

It was found that both catalysts gave the same results, which it may be attributed to the uniform of solid solution at low concentration of Zr (25% mole). Normally, the reactant feed react the reaction on the catalyst surface. So, the uniform of solid solution will complete to corporate the Zr into the ceria lattice and found only ceria on the catalyst surface.

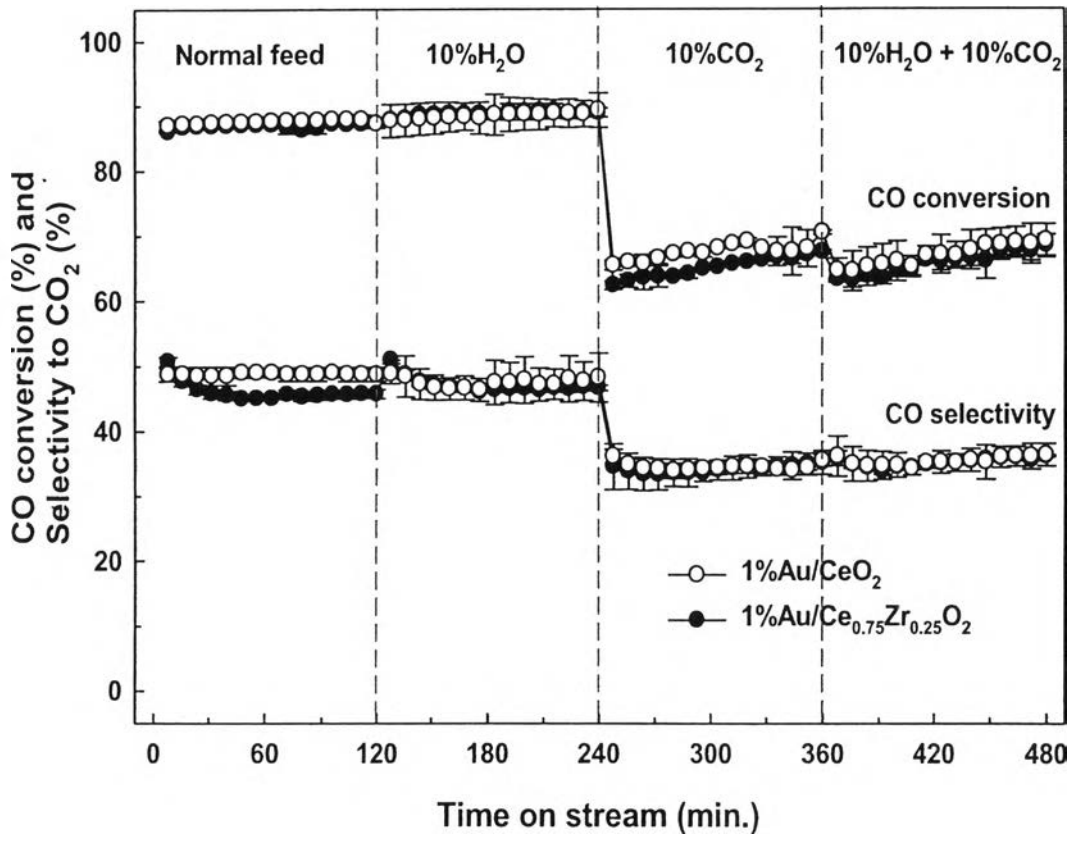

Figure 4.10 The effect of CO_2 and H_2O on the catalytic activities of 1 wt% Au/CeO_2 and 1 wt% $Au/Ce_{0.75}Zr_{0.25}O_2$.The reaction was tested at constant temperature of 110 °C and monitored with time-on-stream.

4.2.3 Effect of Temperature for CO Oxidation Reaction

The catalytic activity of 1 wt% Au/CeO_2 and 1 wt% $Au/Ce_{0.75}Zr_{0.25}O_2$ for low-temperature CO oxidation reaction is shown in Figure 4.11 and 4.12. The reaction was taken in the temperature range 50 to 190 °C under the reaction mixture ratio of $CO:O_2$ for 1:1 and 4:1 in He balanced.

The results show that 1 wt% Au/CeO_2 and 1 wt% $Au/Ce_{0.75}Zr_{0.25}O_2$ can achieve 100% CO conversion in the presence of excess oxygen ($CO:O_2$ = 1:1), whereas

in presence of lean oxygen ($CO:O_2$ = 4:1), 1 wt% $Au/Ce_{0.75}Zr_{0.25}O_2$ catalysts gave a higher catalytic activity than 1 wt% Au/CeO_2 in all range of temperature (Figure 4.12). Because the mixed oxide support possibly supplied the oxygen for the reaction. Thus, 1 wt% $Au/Ce_{0.75}Zr_{0.25}O_2$ provided a higher activity in case of lean oxygen. As compared to CO oxidation reaction and preferential CO oxidation reaction, 1 wt% $Au/Ce_{0.75}Zr_{0.25}O_2$ explicitly exhibited a better performance than 1 wt% Au/CeO_2 in case of CO oxidation reaction. It could be observed that Zr caused to increase oxygen storage capacity and high oxygen mobility. In the presence of excess hydrogen in preferential oxidation reaction had significantly impact effect in the reaction due to it suppressed by competition between H_2 and CO for adsorption and reaction with the activated oxygen atoms (Liotta *et al.*, 2010).

However, the feed stream that obtained from the reformate gas containing excess of hydrogen. Therefore, preferential CO oxidation was an effective technique to get rid of CO concentration from the reformate gas and the catalysts should have stronger CO adsorption than H_2 adsorption.

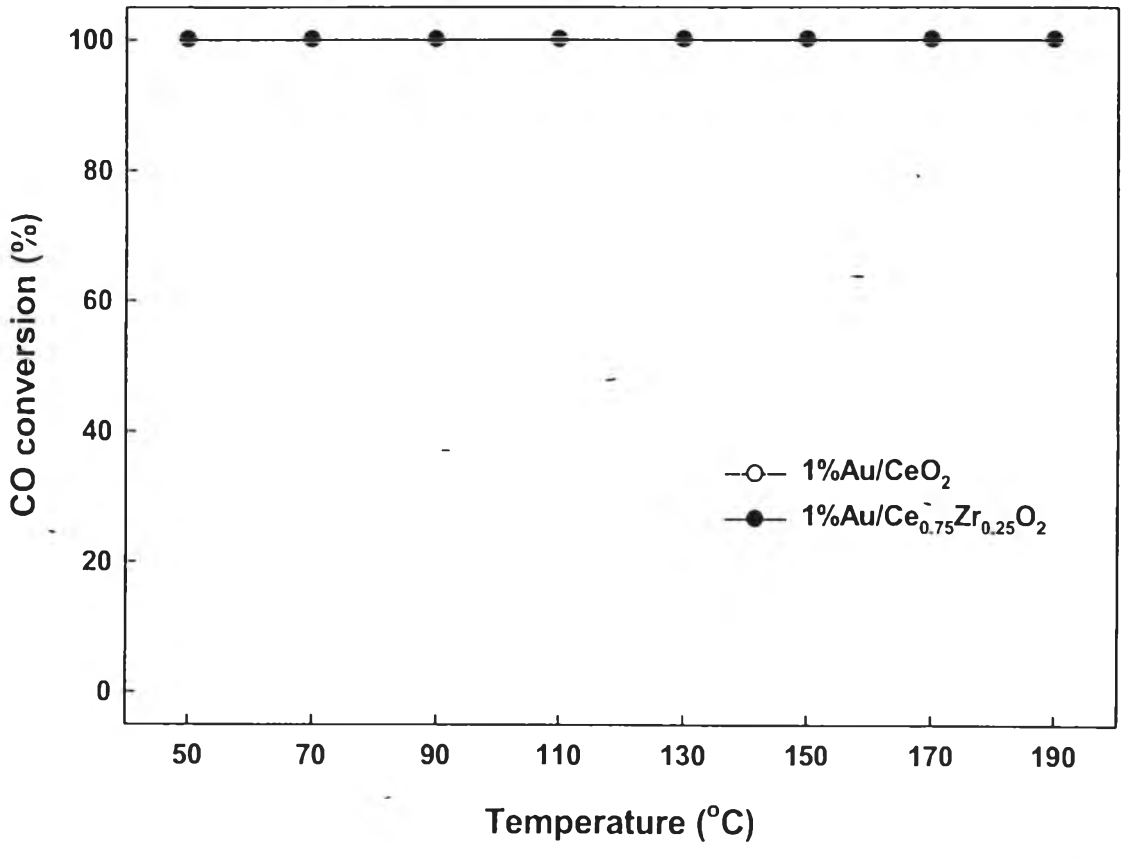

Figure 4.11 CO conversion as a function of reaction temperature for CO oxidation reaction over 1 wt% Au/CeO_2 and 1 wt% $Au/Ce_{0.75}Zr_{0.25}O_2$ catalysts with the reaction mixture of 1% CO, 1% O_2, and He balanced.

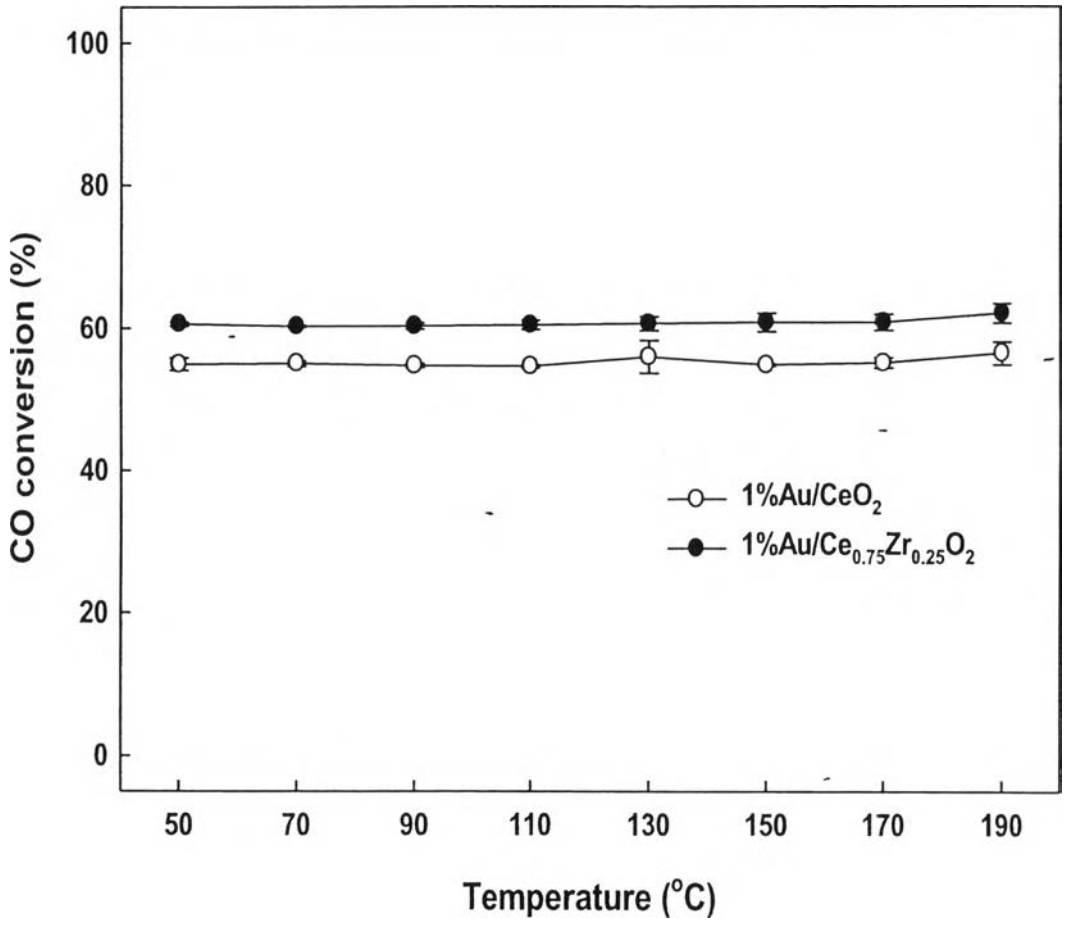

Figure 4.12 CO conversion as a function of reaction temperature for CO oxidation reaction over 1 wt% Au/CeO_2 and 1 wt% $Au/Ce_{0.75}Zr_{0.25}O_2$ catalysts with the reaction mixture of 4% CO, 1% O_2, and He balanced.

4.2.4 Effect of Temperature for Water-Gas Shift Reaction

Figure 4.13 illustrates the catalytic performance of 1 wt% Au/CeO_2 and 1 wt% $Au/Ce_{0.75}Zr_{0.25}O_2$ catalysts for the low temperature water-gas shift (WGS) reaction. The activity was performed with a reactant mixture composition of 4% CO, 10% H_2O and He balanced in the low temperature range of 150–350 °C. The results of

1 wt% Au/CeO_2 and 1 wt% $Au/Ce_{0.75}Zr_{0.25}O_2$ catalysts gave the same trend in the activity, which they obtained the good performance with increasing the temperature due to the viewpoint of kinetics reaction (Vindigni *et al.*, 2012). Moreover, the water-gas shift is an endothermic reaction, which is favorable at high temperature. When comparing between these catalysts, 1 wt% $Au/Ce_{0.75}Zr_{0.25}O_2$ catalysts exhibited higher catalytic performance than 1 wt% Au/CeO_2 at high temperature due to the addition of ZrO_2 could enhance in thermal stability and resistance to sintering (Bedrane *et al.*, 2002). Furthermore, the FTIR results indicated that 1 wt% $Au/Ce_{0.75}Zr_{0.25}O_2$ had low amount of carbonate and several types of differently bound CO molecules on the surface. Thus, these species decreased in the activity and became to block the active sites. The addition of zirconia changed the acid-base properties of the catalyst surface, which the zirconia increased the acid property of ceria. As a consequence the carbonate species was less adsorption in case of acidic surface, as shown in Figure 4.7. Therefore, the activity of the catalyst related to the carbonate-like species because they covered on the support sites and inhibited the CO adsorption (Vindigni *et al.*, 2012).

When comparing water gas shift reaction with preferential CO oxidation reaction, it had higher activity for removal of CO and the activity of mixed oxide support was better at low temperature. In contrast, water gas shift reaction gave a clearly better performance at high temperature reaction and it must be operated at high temperature to achieve the maximum CO conversion (~100% at 350 ^{o}C), whereas preferential CO oxidation reaction can achieve the maximum CO conversion at low temperature (~94% at 50 ^{o}C). Therefore, preferential CO oxidation reaction used low energy consumption and had more efficiency at low temperature.

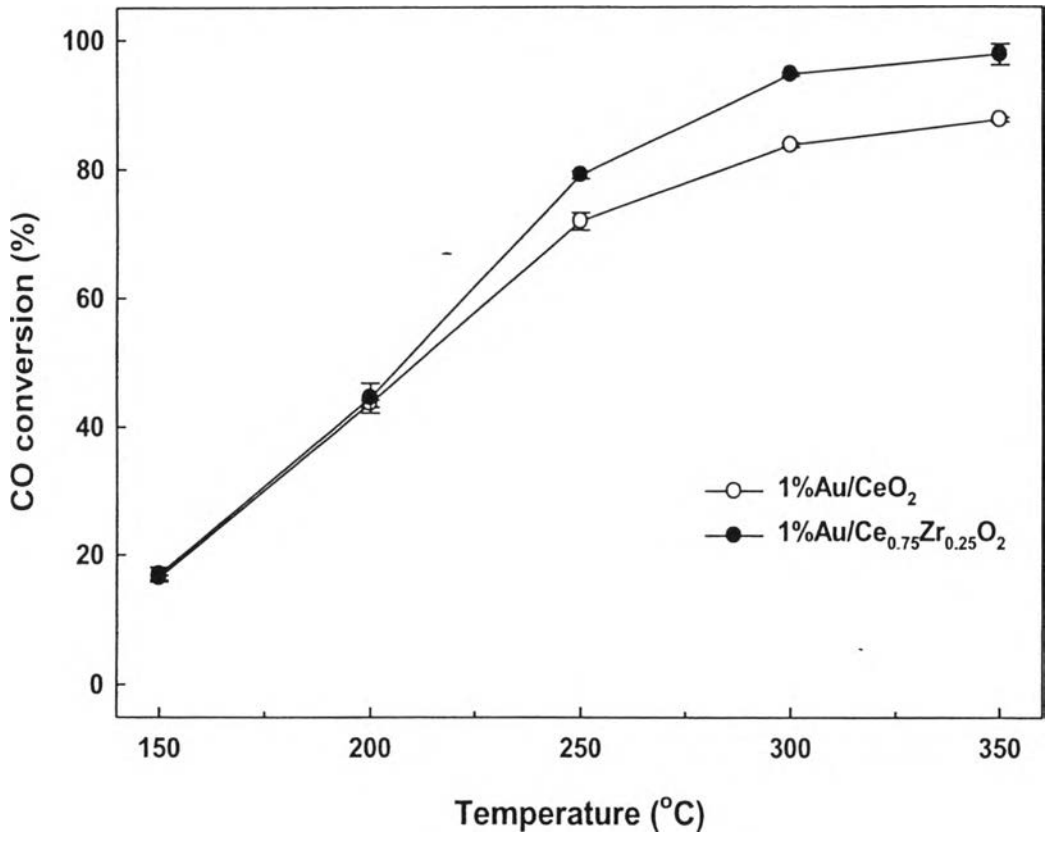

Figure 4.13 CO conversion as a function of reaction temperature for WGS reaction over 1 wt% Au/CeO_2 and 1 wt% $Au/Ce_{0.75}Zr_{0.25}O_2$ catalysts. Reaction mixture: 4% CO, 10% H_2O, and He balanced.

4.2.4 Deactivation Test

The catalytic stability of 1 wt% Au/CeO_2 and 1 wt% $Au/Ce_{0.75}Zr_{0.25}O_2$ catalysts was investigated in dry and wet condition for 33 hours at the temperature of 110 °C, as shown in Figure 4.14. It was found that 1 wt% Au/CeO_2 and 1 wt% $Au/Ce_{0.75}Zr_{0.25}O_2$ catalysts showed the similar results. The results exhibited the good stability in the simulated dry condition. They were maintained for 28 hours without any loss of activity. Then the catalysts were tested for 5 hours in the simulated wet condition and the stability was decreased to 70%, which the deactivation behavior was influenced

by the carbonate and formate species from CO_2 and H_2O. However, they exhibited the same results as the fresh catalysts and were maintained during the reaction time. From the XRD result, there are not changed in the ceria structure and the gold peak cannot be observed. There were a little changed in the crystallite size for both 1 wt% Au/CeO_2 (7.56 to 7.60 nm) and 1 wt% $Au/Ce_{0.75}Zr_{0.25}O_2$ (5.59 to 5.83 nm). Furthermore, the oxygen vacancies increased after exposure the reaction, which these can provide the site for the reaction and lead to the excellent catalytic stability. Nevertheless, the FTIR experiment assigned to the species that could block the active sites after the reaction.

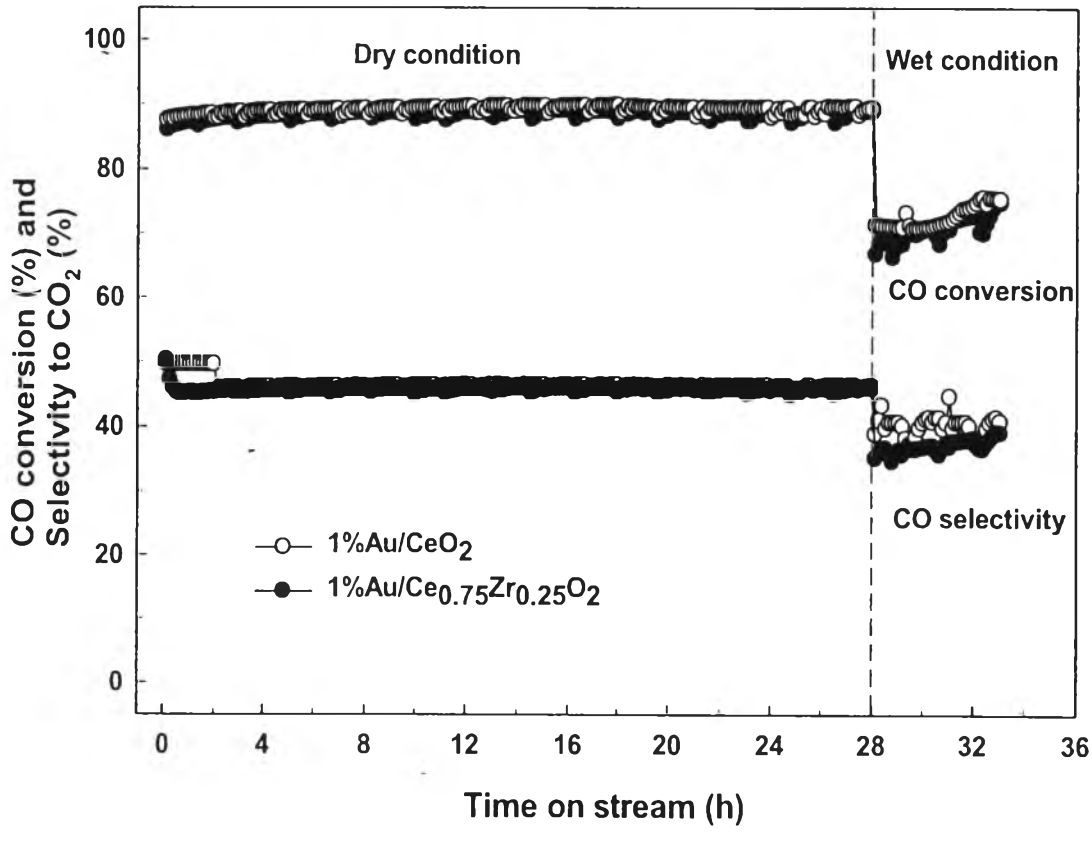

Figure 4.14 Deactivation test of 1 wt% Au/CeO_2 and 1 wt% $Au/Ce_{0.75}Zr_{0.25}O_2$ catalysts. Reaction composition: 1% CO, 1% O_2, 40% H_2 and He balanced for dry condition and 1% CO, 1% O_2, 40% H_2, 10% H_2O, 10% CO_2 and He balanced for wet condition.